



# Effect of acid ( $\text{CH}_3\text{COOH}$ , $\text{H}_2\text{SO}_4$ and $\text{H}_3\text{PO}_4$ ) and basic ( $\text{KOH}$ and $\text{NaOH}$ ) impurities on glycerol valorisation by aqueous phase reforming



J. Remón, C. Jarauta-Córdoba, L. García\*, J. Arauzo

Thermochemical Processes Group (GPT), Aragón Institute for Engineering Research (I3A), Universidad de Zaragoza, Mariano Esquillor s/n, E-50018 Zaragoza, Spain

## ARTICLE INFO

### Article history:

Received 5 May 2017

Received in revised form 10 July 2017

Accepted 24 July 2017

Available online 25 July 2017

### Keywords:

Crude glycerol  
Aqueous phase reforming  
Catalyst deactivation  
Acid impurities  
Basic impurities

## ABSTRACT

This work analyses and compares, under the same operating conditions (220 °C and 44 bar with a Ni-La/ $\text{Al}_2\text{O}_3$  catalyst), the effects of some of the most common acid ( $\text{CH}_3\text{COOH}$ ,  $\text{H}_2\text{SO}_4$ ,  $\text{H}_3\text{PO}_4$ ) and basic ( $\text{KOH}$  and  $\text{NaOH}$ ) biodiesel-derived impurities on the aqueous phase reforming (APR) of a 30 wt.% glycerol solution. The statistical analysis of the results revealed that the impurities did not greatly influence the initial reforming results. Conversely, they significantly influenced the catalyst deactivation, which resulted in different evolutions over time for the glycerol conversion, liquid production and the composition of the gas and liquid phases. Significant decreases over time in the glycerol conversion and liquid production were detected, the severity of the decay being as follows:  $\text{H}_3\text{PO}_4$  ( $\text{KOH} = \text{NaOH}$ ) >  $\text{H}_2\text{SO}_4$  ( $\text{KOH} < \text{NaOH}$ ) >  $\text{CH}_3\text{COOH}$  ( $\text{KOH} < \text{NaOH}$ ). The characterisation of the spent catalyst and the liquid phases revealed that poisoning/fouling, and catalyst active phase or support modification (leaching and crystalline phases alteration), were the major deactivation mechanisms. The proportions of metals (K or Na) deposited on the catalysts with the different acids was as follows:  $\text{H}_3\text{PO}_4$  >  $\text{H}_2\text{SO}_4$  >  $\text{CH}_3\text{COOH}$ . In addition, S and P were also deposited on the catalyst, while boehmite and other new crystalline phases were detected in the spent catalyst after the APR reaction.

© 2017 Elsevier B.V. All rights reserved.

## 1. Introduction

Throughout the world new policies to mitigate global climate change have led researchers to seek new processes, alternative renewable materials and more sustainable strategies to replace the current petroleum-based energy industry with a greener and more environmentally-friendly energy market. Against this background, crude glycerol is of particular interest because of its ample availability as a biodiesel by-product (on average, 1 kg of crude glycerol is yielded with the production of 10 kg of biodiesel) thus converting this feedstock into a cheap resource for which new processes, policies and strategies need to be developed [1].

Given this scenario, different valorisation routes such as gasification, steam reforming, aqueous phase reforming and supercritical reforming have recently been addressed for the production of value-added chemicals and energy from glycerol [2,3]. Among these, Aqueous Phase Reforming (APR), a low temperature, moderate pressure, catalytic process, is a promising route for the valorisation of crude glycerol for the production of value-added

gaseous and liquid chemicals. The gas phase is made up of  $\text{H}_2$ , CO,  $\text{CO}_2$  and  $\text{CH}_4$ , while the liquid phase consists of an aqueous solution containing carboxylic acids, ketones, esters, alcohols and aldehydes. The yields and compositions of the gas and liquid phases depend on the nature of the feed, catalyst, and operating conditions [4–7], allowing the customisation of this valorisation route to suit the different needs of the market.

A substantial number of works in the literature deal with the APR of pure glycerol, addressing the effect of the type of catalyst and the reforming conditions. Noble metal catalysts based on Pt [8–13], Ni [8,9,13–17], Pt–Ni, Cu, Co or Ru [7,8,13,15,18] supported on  $\text{Al}_2\text{O}_3$ ,  $\text{ZrO}_2$ ,  $\text{MgO}$ ,  $\text{SiO}_2$ ,  $\text{CeO}_2$ , or carbon [4,19] and altered, in some cases, with promoters such as La, Ce, Mg and Zr have been synthesised, characterised and tested. In addition, different parametric analyses have been conducted with reagent grade glycerol [11,16,18,20,21]. These studies provide valuable information on the APR process for pure glycerol for both batch and flow reactors. However, the impurities accompanying the crude glycerol obtained from the biodiesel industry can significantly alter the results of the APR of glycerol, modifying the selectivity and causing the deactivation of the catalyst. Therefore, for the development and scale up of this technology, it is essential to know the effects of these impurities on the process.

\* Corresponding author.

E-mail address: [luciag@unizar.es](mailto:luciag@unizar.es) (L. García).

Crude glycerol consists of a mixture of glycerol along with many other problematic impurities such as non-glycerol organic matter, soaps, alcohols, catalysts and salts [1]. To overcome this problem, an initial cost-effective purification of the crude glycerol developed by Manosak et al. [1] was addressed in other works dealing with crude glycerol [22,23]. Briefly, it consists of the physical separation of the FAMES and the elimination of the soaps by an initial acidification, normally with acetic, sulphuric or phosphoric acid, and a subsequent liquid–liquid extraction with a polar solvent such as methanol [1]. As a result, a glycerol solution with 85–90% purity is obtained. This purified glycerol still contains some of the acid used in the neutralization ( $\text{CH}_3\text{COOH}$ ,  $\text{H}_2\text{SO}_4$  or  $\text{H}_3\text{PO}_4$ ), part of the catalyst employed in the biodiesel production (basic such as KOH or NaOH or acid such as  $\text{H}_2\text{SO}_4$  or  $\text{H}_3\text{PO}_4$  [24]) as well as the alcohol (normally  $\text{CH}_3\text{OH}$ ) used during the transesterification reaction and/or in the purification step. Therefore, it is of paramount importance to understand the effects of all these impurities (present either in crude or refined glycerol) on the APR of glycerol.

The works dealing with the APR of crude glycerol are very scarce [4,7,9,25] and only a few of these address the effect of the impurities found in the feedstock. Lehnert and Claus [9] reported the APR of pure and crude glycerol at 250 °C and 20 bar Ar using various Pt catalysts. The presence of NaCl in the glycerol solution was responsible for the lower selectivity to  $\text{H}_2$  and the higher deactivation of the catalyst occurring with crude glycerol. King et al. [4] analysed the APR of a 10 wt.% glycerol/KOH solution using various Pt/C and Re/C catalysts. The increase in the pH of the solution up to 12 by adding 0.1 wt.% of KOH resulted in an increase in the glycerol conversion and the  $\text{H}_2$  production. Boga et al. [25] conducted APR experiments with pure and crude glycerol (6.85 wt.% glycerol, 1.62 wt.% soaps, 1.55 wt.% methanol and 0.07 wt.% esters). The use of this crude glycerol solution resulted in a dramatic depletion in the conversion compared to that of pure glycerol. It was found that fatty acid sodium salts inhibited  $\text{H}_2$  formation to a greater extent than potassium hydroxide. Remón et al. [26] analysed the effect of the presence of different amounts of acetic acid, methanol and potassium hydroxide in a 30 wt.% glycerol solution during APR at 220 °C and 44 bar using a Ni-La/ $\text{Al}_2\text{O}_3$  catalyst. It was found that methanol decreased the glycerol conversion while acetic acid and potassium hydroxide inhibited and potentiated the gas production, respectively. Potassium hydroxide promoted  $\text{H}_2$  production due to the greater gas formation and the lower  $\text{H}_2$  consumption. As regards liquid production, methanol increased the relative amount of monohydric alcohols in the liquid, while potassium hydroxide did not greatly vary the liquid product distribution. Acetic acid promoted dehydration reactions, which led to a decrease in the proportion of monohydric alcohols and an increase in the relative amount of ketones made up of three carbon atoms.

These publications provide valuable information about the presence of some of the most common impurities found in crude and refined glycerol. However, since different feedstocks, catalysts, reactors and operating conditions were used, the comparison between the effects of the different impurities in the process is unreliable. Given this scenario, this work analyses and compares under the same operating conditions (220 °C and 44 bar using a Ni-La/ $\text{Al}_2\text{O}_3$  catalyst) the effects of some of the most common acid and basic impurities found in crude and purified glycerol:  $\text{CH}_3\text{COOH}$ ,  $\text{H}_2\text{SO}_4$ ,  $\text{H}_3\text{PO}_4$ , KOH and NaOH. These operating conditions were used in our previous work [26], thus allowing a deeper insight into the APR of crude glycerol to be gained. The effects of these impurities have been analysed on the glycerol conversion, the product distribution in carbon basis and the compositions of the gas and liquid phases. In addition, the spent catalyst was exhaustively characterised by several techniques, which allowed a relationship to be established between the impurities and both the APR results and catalyst deactivation. Given the fact that the effect of the presence

in crude glycerol of all these acid and basic impurities under the same operating conditions has never been addressed before, and considering the limited number of publications dealing with crude glycerol along with the scarce number of publications analysing catalyst deactivation in APR, this innovative work not only provides a better insight into the APR of crude glycerol, but will also lead to a greater understanding and consequently prevention of the most common catalyst deactivation mechanisms during this thermochemical process.

## 2. Experimental

### 2.1. Aqueous phase reforming rig

The experiments were conducted in a continuous pressurised fixed bed reactor for 3 h using a Ni-La/ $\text{Al}_2\text{O}_3$  catalyst. The experimental facility is a “microactivity unit” designed and built by PID (Process Integral Development Eng & Tech, Spain). It consists of a stainless steel pressurised fixed bed reactor (9 mm inner diameter) heated up by means of an electric furnace. The system pressure, measured with a pressure gauge located at the exit of the reactor, is reached with the aid of an automatic micrometric valve operated by a rotor. The aqueous solutions containing the glycerol and impurities are fed into the reactor from its bottom part by using a high performance liquid chromatography (HPLC) pump. The liquids (unreacted reactants and reaction products) together with the gases produced during the reaction leave the reactor from its upper part, pass through the micrometric valve and arrive at the condensation system. This consists of a set of three condensers where the liquids are separated from the gas mixture ( $\text{N}_2$  used as an internal standard and the gases produced) at intervals of 1 h to analyse the evolution over time of the liquid phase. A micro gas chromatograph (Micro GC) equipped with thermal conductivity detectors (TCD) was used for the online analysis of the gas phase. The liquid samples were collected and analysed offline with a gas chromatograph equipped with Flame Ionization (FID) and Mass Spectrometry (MS) detectors. More detailed information about the experimental unit and the catalyst properties can be found in our previous communications [22,26,27].

### 2.2. Experimental plan, response variables and data analysis

The influence of the presence of some common glycerol biodiesel-derived acid ( $\text{CH}_3\text{COOH}$ ,  $\text{H}_2\text{SO}_4$  and  $\text{H}_3\text{PO}_4$ ) and basic (KOH and NaOH) impurities has been investigated during the aqueous phase reforming of a water solution containing 30 wt.% glycerol and 2.5 wt.% methanol. Table 1 shows the pH of the solutions and the concentrations of the acids ( $\text{CH}_3\text{COOH}$ ,  $\text{H}_2\text{SO}_4$ ,  $\text{H}_3\text{PO}_4$ ) and bases (KOH and NaOH) used to prepare them. The concentration of methanol was chosen having regard to the glycerol/methanol ratio found in biodiesel-derived refined glycerol solutions [1,28] and previously described in our previous communication [26] in order to gain a reliable insight into the effects of these impurities on crude/refined glycerol APR, while the concentrations of the acid and basic impurities were selected to have the same concentration

**Table 1**

Concentrations of acid and basic impurities (wt.%) and pH of the solutions used in the APR experiments.

Run	$\text{CH}_3\text{COOH}$	$\text{H}_2\text{SO}_4$	$\text{H}_3\text{PO}_4$	KOH	NaOH	pH
1	1.5	0	0	1.4	0	$6.80 \pm 0.06$
2	1.5	0	0	0	1.0	$7.09 \pm 0.19$
3	0	1.0	0	1.4	0	$7.25 \pm 0.16$
4	0	1.0	0	0	1.0	$7.08 \pm 0.26$
5	0	0	1.9	1.4	0	$6.75 \pm 0.06$
6	0	0	1.9	0	1.0	$6.83 \pm 0.22$

of  $H^+$  and  $OH^-$  (same pH) in all the solutions as those reported for  $CH_3COOH$  [26].

The aqueous phase reforming experiments were conducted at 44 bar and 220 °C with a Ni-La/ $Al_2O_3$  catalyst using a spatial time defined as the mass of catalyst/mass flow rate of glycerol ( $W/m_{glycerol}$ ) ratio of 25 g catalyst min/g glycerol and a liquid flow rate of 1 mL/min [26]. The catalyst was prepared by coprecipitation, having a 28% (relative atomic percentage) of Ni expressed as Ni/(Ni + Al + La), an atomic La/Al ratio of 0.035 and a BET surface area of 187  $m^2/g$ . It was activated (reduced) in situ previously to the APR reaction using a  $H_2$  flow rate of 100 mL (STP)/min at 650 °C for 1 h. The response variables studied were the global glycerol conversion ( $X_{gly}$ ), the carbon conversion to gas, liquids and solid (CC gas, CC liq and CC sol) as well as the composition of the gas ( $N_2$  and  $H_2O$  free, vol.%) and liquid (relative chromatographic area free of water and un-reacted glycerol, %). More information about the response variables and the analytical methods used for their calculation can be found in our previous communications [22,26]. In addition, Inductive Coupled Plasma Optical Emission Spectrometry (ICP-OES) was used to measure the amount of metals leached from the catalyst to the liquid phase. To do this, a liquid sample containing equal amounts of the liquids produced during the 1st, 2nd, and 3rd hours of experiment was prepared and analysed.

The experimental results for each response variable are divided into three intervals, which correspond to the average value of each variable obtained during the first, second and third hour of the experiment. All the experiments were conducted at least in duplicate and the influence of each impurity in the process has been analysed using a one-way analysis of variance (one-way ANOVA) with 95% confidence. Furthermore, Fisher's least significant difference (LSD) test was used to compare pairs of data, i.e. either to analyse the effect of the reaction time (comparing the responses for the same experiment) or the effect of the impurities between dif-

ferent experiments. The LSD test results are presented graphically by means of LSD bars. Significant differences (with 95% confidence) between any pair of data can be ensured when their LSD bars do not overlap.

### 2.3. Characterisation of the catalyst after reaction

The spent catalyst was characterised by elemental (CHNS) and thermo gravimetric (TG) analyses, X-Ray diffraction (XRD) and Inductive Coupled Plasma Optical Emission Spectrometry (ICP-OES). TG analyses were conducted under a  $N_2$  atmosphere from 25 °C to 600 °C at a heating rate of 10 °C/min, monitoring the weight loss of the samples. XRD patterns of the original and the spent catalysts were obtained with a D-Max Rigaku diffractometer equipped with a  $CuK\alpha 1.2$  at a tube voltage of 40 kV and current of 80 mA using continuous-scan mode with steps of 0.03°/s at Bragg's angles ( $2\theta$ ) ranging from 5° to 85°. The phases present in the samples were defined with reference to the JCPDS-International Centre for Diffraction Data 2000 database.

### 2.4. Possible reactions during the APR of glycerol

Glycerol APR comprises the formation of gases and liquids. Three possible parallel routes explain the formation of liquid products: glycerol dehydration to 1-hydroxypropan-2-one (A) [4,5,18,29–32] and/or to 3-hydroxypropanal (B) [5,30–32] and/or glycerol dehydrogenation to 2,3-dihydroxypropanal (C) [4,5,18,29–32]. This mechanism has been thoroughly discussed in our previous communications [22,26]. The gas phase is made up of a mixture of  $H_2$ ,  $CO_2$ ,  $CO$  and  $CH_4$ . The thermal decomposition and/or reforming reactions of the glycerol and all the liquid intermediates ( $C_nH_mO_k + (n-k) H_2O \rightleftharpoons n CO + (n+m/2-k) H_2$ ) as well as the decarbonylation reactions are responsi-

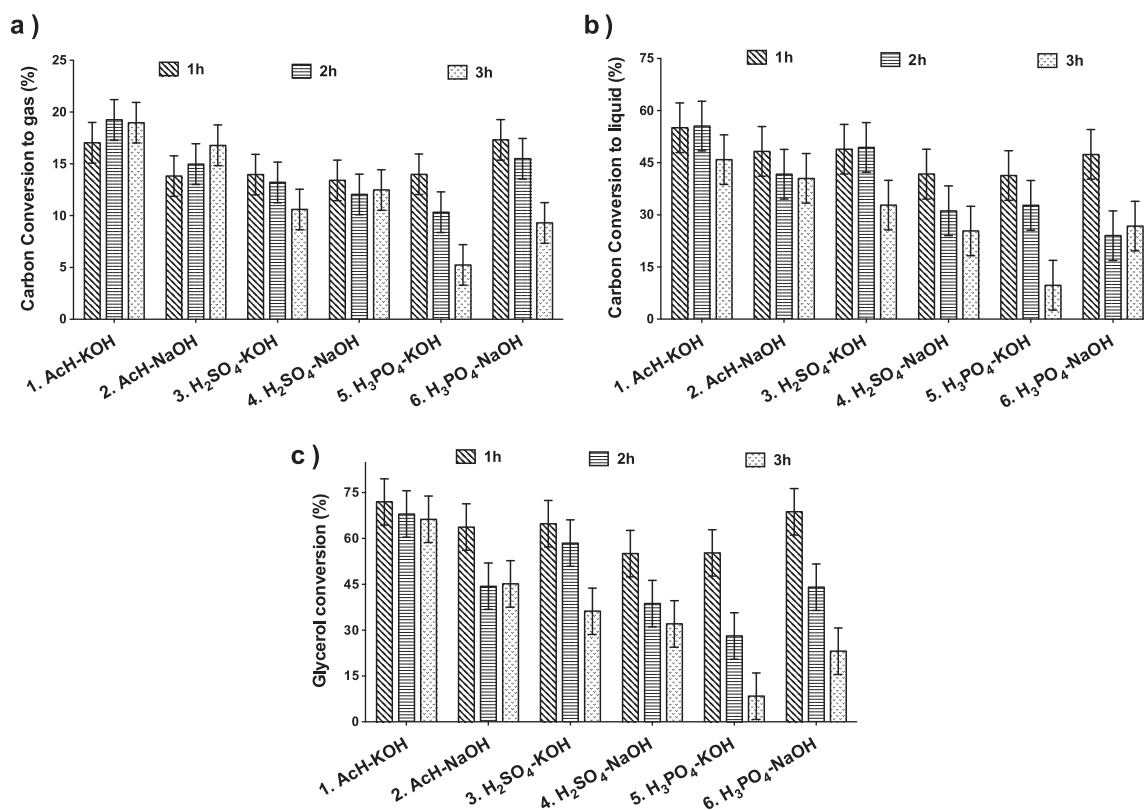


**Fig. 1.** Glycerol APR products distribution in carbon basis (CC gas and CC liq) and glycerol conversion. Results are expressed as mean  $\pm$  0.5 Fisher LSD intervals with 95% confidence.

ble for the formation of  $H_2$  and CO while the water gas shift reaction ( $CO + H_2O \rightleftharpoons CO_2 + H_2$ ) and methanation reactions ( $CO + 3H_2 \rightleftharpoons CH_4 + H_2O$  and  $CO_2 + 4H_2 \rightleftharpoons CH_4 + 2H_2O$ ) account for the presence of  $CO_2$  and  $CH_4$  in the gas phase [4,5,18,29–32].

### 3. Results

#### 3.1. Glycerol conversion and C product distribution (CC gas, CC liq and CC sol)

Fig. 1 shows the carbon converted to gas and liquid (CC gas, CC liq) along with the global conversion of glycerol (X gly). Statistically significant differences between the results obtained in the experiments were found for the CC gas, CC liq and X gly (p-values < 0.001) with variations between 5 and 19%, 10–55% and 8–72%, respectively. The CC sol was lower than 5% in all cases and the effect of the impurities on the CC sol was not significant (p-value > 0.05). The effects of the type of acid and base for these variables have been analysed comparing the results obtained during the first hour of reaction (initial values) and the evolution of these variables over time to examine a possible catalyst deactivation and/or changes in the reaction pathway.

The statistical analysis of the results reveals that the type of acid and base does not significantly influence the initial global results; i.e. the values obtained for the CC gas, CC liq and X gly during the first hour of experiment with the different acids ( $CH_3COOH$ ,  $H_2SO_4$  or  $H_3PO_4$ ) and bases (KOH or NaOH) are not statistically different (p-value > 0.05). These results are the consequence of having used the same pH to prepare the solutions [26] and suggest that the presence of different amounts of S, P, Na or K in the solution does not exert a significant influence on the initial global results during the APR of glycerol under the experimental conditions tested in this work.

Conversely, the impurities exert a significant influence on the evolution over time of these variables. Specifically, significant decreases occur for the X gly and the CC liq; the variations observed for the CC gas being less marked. These developments suggest a possible catalyst deactivation, which does not influence gas production in some cases. Specifically, the variations observed for the CC gas depend on the type of acid. More precisely, while non-significant variations occur with  $CH_3COOH$  or  $H_2SO_4$  (either accompanied by KOH or NaOH), a sharp decrease in the CC gas over time takes place when  $H_3PO_4$  is present in the solution, regardless of the base. This development suggests that in this case  $H_3PO_4$  is responsible for the decrease observed in the gas production. The evolution over time for the CC liq shows significant decreases in some cases. While non-significant variations occur with  $CH_3COOH$  in the solution (either with KOH or NaOH), a moderate and a sharp decay occur with  $H_2SO_4$  and  $H_3PO_4$ , respectively. For  $H_3PO_4$ , a sharper decrease takes place in the presence of KOH than with NaOH. This suggests a synergetic acid-base interaction that might lead to an increase in the deactivation of the catalyst. The glycerol conversion shows significant decreases over time in most of the experiments. Both the types of acid and base influence the evolution over time of the X gly. Regardless of the type of base (KOH or NaOH), the decreases for the X gly are as follows:  $CH_3COOH$  (KOH < NaOH) <  $H_2SO_4$  (KOH < NaOH) <  $H_3PO_4$  (KOH = NaOH).

#### 3.2. Gas composition

Fig. 2 shows the gas composition obtained with the different acids and bases considered in this work. The analysis of the results reveals a statistically significant influence (p-values < 0.05) of the impurities on the relative amounts of  $H_2$ ,  $CO_2$ , CO and  $CH_4$  in the gas. The greatest variations occur for the relative amounts of  $H_2$  (29–44 vol.%) and  $CH_4$  (15–22 vol.%); the variations occurring for  $CO_2$  (38–46 vol.%) and CO (1–3 vol.%) are less marked and irrelevant

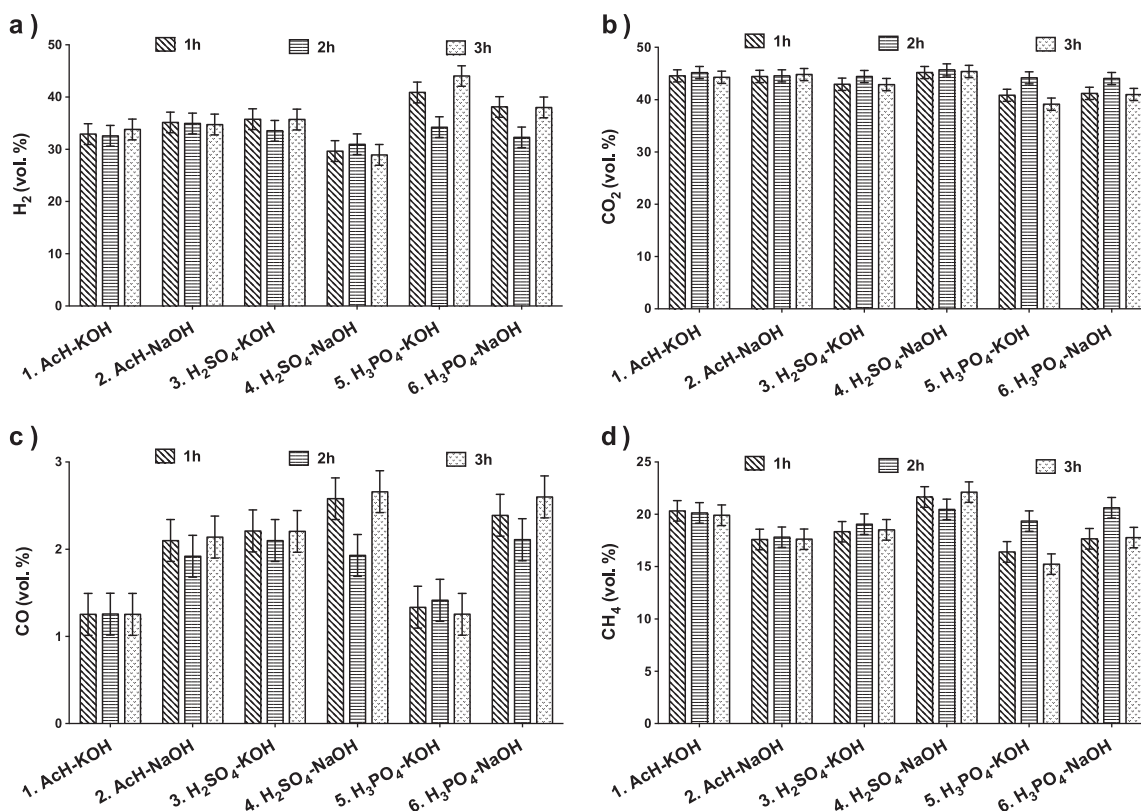


Fig. 2. Composition of the gas phase (vol.%). Results are expressed as mean ± 0.5 Fisher LSD intervals with 95% confidence.



from a practical point of view. In addition, the statistical analysis reveals that the impurities exert different effects on the initial composition of the gas phase. Specifically, the relative amounts of  $H_2$  and  $CH_4$  are more affected by the presence of the different types of acids and bases than the proportions of  $CO$  and  $CO_2$ . For these two latter gases, although the variations observed are statistically significant, they are not practically important.

A multivariate analysis by means of Spearman's test was carried out for the relative amounts of  $H_2$ ,  $CO_2$ ,  $CO$  and  $CH_4$  in the gas. This test revealed a statistically significant relationship between the proportions of  $H_2$  and  $CO_2$  ( $p$ -value = 0.0001;  $R^2$  = 0.91) and the proportions of  $H_2$  and  $CH_4$  ( $p$ -value = 0.0001;  $R^2$  = 0.94). This indicates that the impurities considered exert a significant influence on the methanation reaction ( $CO_2 + 4H_2 \rightleftharpoons CH_4 + 2H_2O$ ) and the WGS ( $CO + H_2O \rightleftharpoons CO_2 + H_2$ ) reactions. These variations depend on the type of acid and base considered. The highest proportion of  $H_2$  in the gas along with the lowest concentration of  $CH_4$  is obtained with  $H_3PO_4$ , in the presence of either  $KOH$  or  $NaOH$ . A lower proportion

of  $H_2$  together with a higher relative amount of  $CH_4$  in the gas is produced with  $H_2SO_4$  and  $NaOH$  in the glycerol solution.

The evolution of the gas over time shows small variations in the composition of the gas. This indicates that catalyst deactivation does not greatly affect gas selectivity, i.e. lower amounts of all the gases are produced but the composition of the gas is not altered. This development was reported in our previous work analysing the influence of  $CH_3OH$ ,  $CH_3COOH$  and  $KOH$  during the APR of a 30 wt.% glycerol solution with the same catalyst and under the same operating conditions [26]. The greatest variation in the gas composition occurs for  $H_3PO_4$ . For this acid, regardless of the type of base used, an initial decay followed by a posterior increase in the proportion of  $H_2$  in the gas takes place. This development occurs along with contrasting variations in the amounts of both  $CO_2$  and  $CH_4$ . The increases in the  $H_2$  content in the gas from the second to the third hour could be accounted for by a lesser spread of hydrogenation reactions due to the progressive deactivation of the catalyst; thus increasing the proportion of  $H_2$  in the gas [22,26].

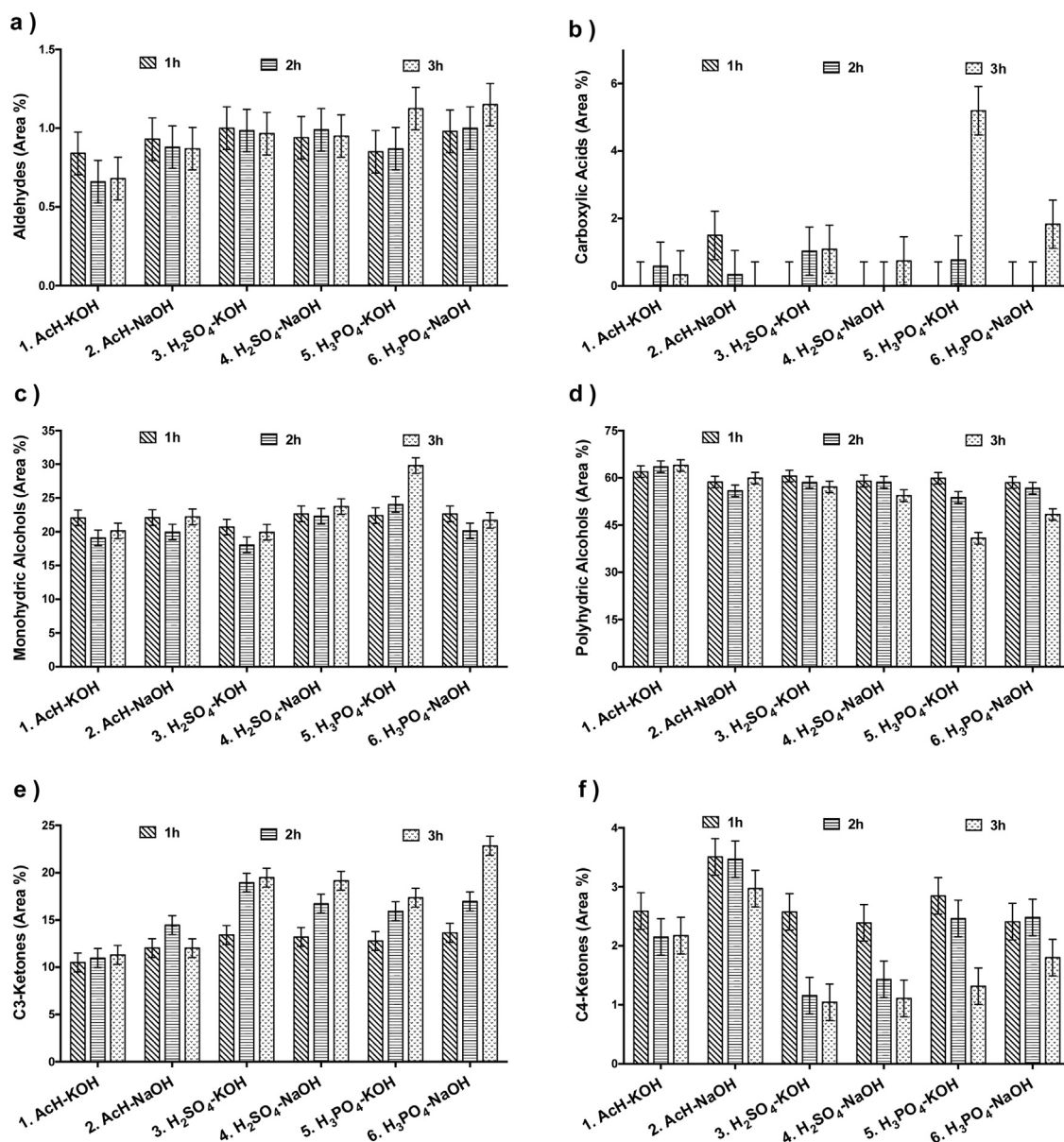


Fig. 3. Composition of the liquid phase (relative chromatographic area, %). Results are expressed as mean  $\pm$  0.5 Fisher LSD intervals with 95% confidence.

**Table 2**

Relative amounts of active phase metals leached to the liquid phase during the APR experiments. Results are presented as mean  $\pm$  standard deviation.

Run	Ni leached (%)	Al leached (%)	La leached (%)
1. AcH – KOH	0.0065 $\pm$ 0.002	0.026 $\pm$ 0.03	2.55 $\pm$ 1.40
2. AcH – NaOH	0.005	0.0024	2.81
3. H <sub>2</sub> SO <sub>4</sub> – KOH	0.012	0.021	0.022
4. H <sub>2</sub> SO <sub>4</sub> – NaOH	0.017	0.023	0.060
5. H <sub>3</sub> PO <sub>4</sub> – KOH	0.009 $\pm$ 0.001	0.017 $\pm$ 0.004	0.084 $\pm$ 0.014
6. H <sub>3</sub> PO <sub>4</sub> – NaOH	0.015 $\pm$ 0.013	0.015 $\pm$ 0.012	0.01 $\pm$ 0.098
p-value	0.8018	0.9878	0.1410

### 3.3. Liquid composition

The relative amounts of the chemical families detected in the liquids are shown in Fig. 3. The liquid phase consists of a mixture of aldehydes, carboxylic acids, alcohols and ketones along with unreacted glycerol and water. Acetaldehyde and acetic acid are the most abundant compounds for the aldehydes and carboxylic acids, respectively. The alcohols mostly comprise monohydric (methanol and ethanol) and polyhydric (propane-1,2-diol, ethane-1,2-diol and butane-2,3-diol) alcohols. The ketones include C3-ketones such as propan-2-one (acetone) and 1-hydroxy-propan-2-one and C4-ketones such as 3-hydroxy-butan-2-one. The presence of these compounds in the condensates is consistent with the pathway proposed in our previous works [22,26], and those proposed by several authors who have studied the APR of glycerol [4,5,18,29–32]. In addition, CH<sub>3</sub>O<sup>−</sup>, which has a mid nucleophilic character, can be formed in the presence of CH<sub>3</sub>OH and KOH/NaOH [33], and can promote the formation of alcohols and ketones with a higher number of carbon atoms via Cannizzaro type reactions [5,30–32].

The statistical analysis reveals that the impurities exert different effects on the composition of the liquid phase. Specifically, the initial amounts (1st h) for the different families of compounds are not statistically affected by the presence of the impurities in the glycerol solution (p-value > 0.05). The initial composition of the liquid phase shifts as follows: aldehydes (0.84–1%), carboxylic acids (0–1.5%), monohydric alcohols (21–23%), polyhydric alcohols (59–61%), C3-ketones (11–14%) and C4-ketones (2–4%). Conversely, the impurities exert a significant influence on the composition of the liquid phase over time. Significant variations take place for the proportions of alcohols and ketones; the variations observed for the relative amounts of aldehydes and carboxylic acids are less important from a practical point of view due to the small proportion of these two families in the liquids.

These variations over time depend on the type of acid. While significant variations do not take place in the presence of CH<sub>3</sub>COOH, minor and great changes in the proportions of alcohols and ketones occur with H<sub>2</sub>SO<sub>4</sub> and H<sub>3</sub>PO<sub>4</sub>, respectively. Among these, the greatest variations take place for the proportions of polyhydric alcohols and ketones in the presence of H<sub>3</sub>PO<sub>4</sub>. Specifically, decreases over time occur for the proportions of polyhydric alcohols and C4-ketones in the liquid, while C3-ketones show increases over time. These developments depend on the type of base, and more pro-

nounced variations occur with KOH than with NaOH, except for the C3-ketones. The changes observed in the presence of H<sub>2</sub>SO<sub>4</sub> are less marked; a small depletion occurs in the proportion of polyhydric alcohols along with an increase and a reduction in the relative amounts of C3-ketones and C4-ketones, respectively. In this case, these developments do not depend on the type of base and the same variations are observed with either KOH or NaOH. The variations in the proportions of polyhydric alcohols and C3-ketones account for the decrease in the proportion of propane-1,2-diol and the increase in the relative amount of 1-hydroxypropan-2-one, respectively. These developments indicate that catalyst deactivation hinders hydrogenation reactions in route A [22,26]. Route A comprises a dehydration reaction to produce 1-hydroxypropan-2-one, occurring in the acid centres of the catalyst [34,35], followed by a hydrogenation reaction to produce propane-1,2-diol, for which metallic centres are needed [35]. Therefore, this development is believed to be a consequence of the deactivation of the metal active centres in the catalyst.

### 3.4. Characterisation of the spent catalysts

To gain a better insight into the effects of the impurities on the process (initial values for the response variables and their evolution over time), the liquid phase produced and the spent catalysts were thoroughly characterised by different analytical techniques. This characterisation aims to elucidate the causes of the different evolutions over time for the response variables considered. These could be a consequence of catalyst deactivation by coking, poisoning/fouling, and/or catalyst active phase or support modification (leaching and phase transformation). Specifically, elemental (CHNS) and thermo gravimetric (TG) analyses and X-Ray diffraction (XRD) were used for the characterisation of the spent catalysts while Inductive Coupled Plasma Optical Emission Spectrometry (ICP) was used for both the spent catalyst and the liquid phase.

As regards leaching, the ICP analysis of the liquid phases revealed the presence of Ni, Al and La in the liquids. Table 2 lists the relative amounts (total mass of metal leached during the 3 h reaction with respect to the total amount of metal loaded in the catalyst and used in the experiment, %) of metals leached from the catalyst to the liquid phase during the APR reactions. The proportions are relatively low, especially for the amounts of Ni and Al, the amount of La being slightly higher. However, very interestingly, the statistical analysis of the results reveals that the type of acid and base does not exert a significant influence (p-value > 0.05) on leaching under the operating conditions used in this work. This is believed to be a consequence of having used the same pH to prepare the solutions employed in the experiments. These results also suggest that leaching is not responsible for the different reforming results observed in this work. This development is in agreement with our previous study [26] and with the results reported by other authors [36,37] in which it was found that leaching depends on the pH of the solution.

With respect to coking and poisoning, Table 3 shows the amounts of C, K, Na, S and P deposited on the spent catalysts cal-

**Table 3**

Amounts of impurities (X = C, K, Na, S and P) deposited on the catalyst during the APR experiments expressed as mg X/g cat g X fed. Results are presented as mean  $\pm$  standard deviation.

Run	C	K	Na	S	P
1. AcH – KOH	0.25 $\pm$ 0.01 <sup>a</sup>	4.67 $\pm$ 0.47 <sup>c</sup>			
2. AcH – NaOH	0.28 $\pm$ 0.01 <sup>a</sup>		6.28 $\pm$ 0.02 <sup>c</sup>		
3. H <sub>2</sub> SO <sub>4</sub> – KOH	0.28 $\pm$ 0.01 <sup>a</sup>	19.87 $\pm$ 0.19 <sup>b</sup>		48.26 $\pm$ 0.07 <sup>a</sup>	
4. H <sub>2</sub> SO <sub>4</sub> – NaOH	0.19 $\pm$ 0.01 <sup>b</sup>		6.57 $\pm$ 0.04 <sup>b</sup>	23.18 $\pm$ 0.12 <sup>b</sup>	
5. H <sub>3</sub> PO <sub>4</sub> – KOH	0.18 $\pm$ 0.02 <sup>b</sup>	31.95 $\pm$ 0.76 <sup>a</sup>			70.58 $\pm$ 0.74 <sup>a</sup>
6. H <sub>3</sub> PO <sub>4</sub> – NaOH	0.26 $\pm$ 0.01 <sup>a</sup>		11.62 $\pm$ 0.06 <sup>a</sup>		0.79 $\pm$ 0.01 <sup>b</sup>

a, b and c in each column represents statistically significant groups with 95% confidence.

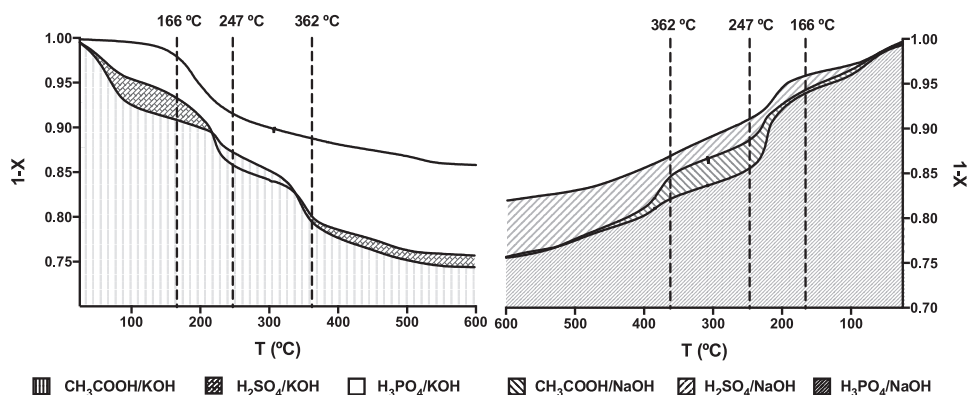


Fig. 4. TG analysis for the spent catalysts employed in the APR experiments.

culated from the elemental and ICP analyses of the used catalyst. The amount of C deposited on the catalyst surface was lower than 0.28 mg C/g catalyst g of C for all the experiments. This suggests that carbon deposition on the catalyst surface under the experimental conditions tested is negligible. In addition, although statistically significant variations are detected for the amount of C deposited on the catalysts, they are not important from a practical point of view. This suggests that catalyst deactivation by coking is not the main process responsible for the decreases observed in some of the response variables over time. Similar results were reported in previous works in which this catalyst was also used for the APR of different organic feedstocks (crude glycerol, lactose and cheese whey) [22,26,27,38]. In addition, it should be borne in mind that part of the C deposited on the catalyst can be accounted for by the formation of  $\text{LaCO}_3\text{OH}$  (XRD analysis) and therefore the amount of C quantified in the spent catalyst might include both coke and  $\text{LaCO}_3\text{OH}$  formation.

Conversely, significant variations were detected in the amounts of K, Na, S and P deposited on the catalysts. The amounts of K and Na deposited on the catalyst statistically depend on the type of acid employed during the experiments and the following trend is observed:  $\text{H}_3\text{PO}_4 > \text{H}_2\text{SO}_4 > \text{CH}_3\text{COOH}$ . This trend coincides with the decay observed for the carbon conversion to liquid, the glycerol conversion and the variations observed in the composition of the liquid phase. As regards S and P, a greater amount of these compounds is deposited in the experiments conducted with KOH than with NaOH. This development could explain the more pronounced decay in the carbon conversion to liquid and the glycerol conversion observed for the former than for the latter base.

These results indicate that the deposition of K on the catalyst might have two different effects on the deactivation of the catalyst. On the one hand, it can increase the catalytic activity as can be observed for the experiments conducted with  $\text{CH}_3\text{COOH}$ . This is in agreement with the work of King et al. [4], who also reported the positive effect of K in the APR of glycerol and suggested that K could benefit the catalytic activity by making the active metal phase of the catalyst more electron-deficient, thus increasing its Lewis acidity. In addition, in a previous work using this catalyst [26], we also reported the positive effect of K during the APR of glycerol. On the other hand, K deposition aids the deposition of S and P due to the higher electro deficiency of the catalyst; thus contributing to catalyst deactivation. A synergistic effect between K and S or P can be observed; i.e. a greater K deposition occurs in the presence of S or P and a larger deposition of these two elements takes place with K than with Na. However, when comparing the experiments conducted with KOH and NaOH, the decreases observed in the catalytic activity are not proportional to the amounts of S and P deposited and significant differences are not observed. This could be the con-

sequence of the positive effect of K on the activity of the catalyst, which can compensate for the negative effect of S and P.

Regarding phase transformation, Figs. 4 and 5 show the characterisation results of the spent catalysts by TG and XRD, respectively. The TG analysis displays four decomposition steps (25–166 °C; 166–247 °C; 247–362 °C and 362–600 °C), which correspond to the decomposition of boehmite into alumina [39–41] involving the loss of physisorbed (I) and chemisorbed water (II), boehmite conversion into transition alumina (III), and transition alumina dehydration (IV). The experimental temperature intervals for the decomposition of the used catalysts are fairly similar to those reported for pure boehmite and those reported in a previous work with the same catalyst under similar operating conditions [22], the incorporation of different metals on the catalyst structure being responsible for the small differences [41].

From the experimental results it can be observed that the type of acid and base exerts a significant influence on boehmite formation according to the TG analyses. In particular, boehmite formation in the presence of KOH is as follows:  $\text{CH}_3\text{COOH} = \text{H}_2\text{SO}_4 > \text{H}_3\text{PO}_4$ ; while the following trend is observed when NaOH is used:  $\text{CH}_3\text{COOH} = \text{H}_3\text{PO}_4 > \text{H}_2\text{SO}_4$ . Very interestingly, similar boehmite formation occurs for  $\text{CH}_3\text{COOH}$  regardless of the base used, whilst for  $\text{H}_2\text{SO}_4$  and  $\text{H}_3\text{PO}_4$  boehmite formation depends on the type of base. While a greater boehmite formation takes place with KOH than with NaOH for  $\text{H}_2\text{SO}_4$ , the opposite trend is observed for  $\text{H}_3\text{PO}_4$ ; i.e. a greater boehmite formation with NaOH than with KOH. This development suggests a significant acid-base interaction, which can affect boehmite formation under the operating conditions used in this work.

Under hydrothermal conditions, boehmite formation depends on the temperature, pH and presence of inorganic impurities/molecules in the solution [42]. In the present work the experiments were conducted at the same operating conditions (220 °C and 44 bar) and the solutions were prepared to have the same pH (6.8–7.1). This suggests that the differences observed in boehmite formation occurring in this work could be the consequence of the presence of S and P in the solutions. The highest boehmite formation occurs with  $\text{CH}_3\text{COOH}$  (in the absence of S or P), the presence of these two compounds inhibiting boehmite formation. This inhibiting effect depends on the presence of K and Na in the solutions with two opposing results: while S inhibits boehmite formation in the presence of Na, P hinders it when K is in the solution. This difference could be the consequence of the formation of different water-soluble S and P complexes with K rather than with Na, thus decreasing the effective amounts of S and P in the solutions to inhibit boehmite formation.

In all cases, the highest boehmite formation occurs with  $\text{CH}_3\text{COOH}$  regardless of the type of base. However, this development is not in good agreement with the less pronounced variations

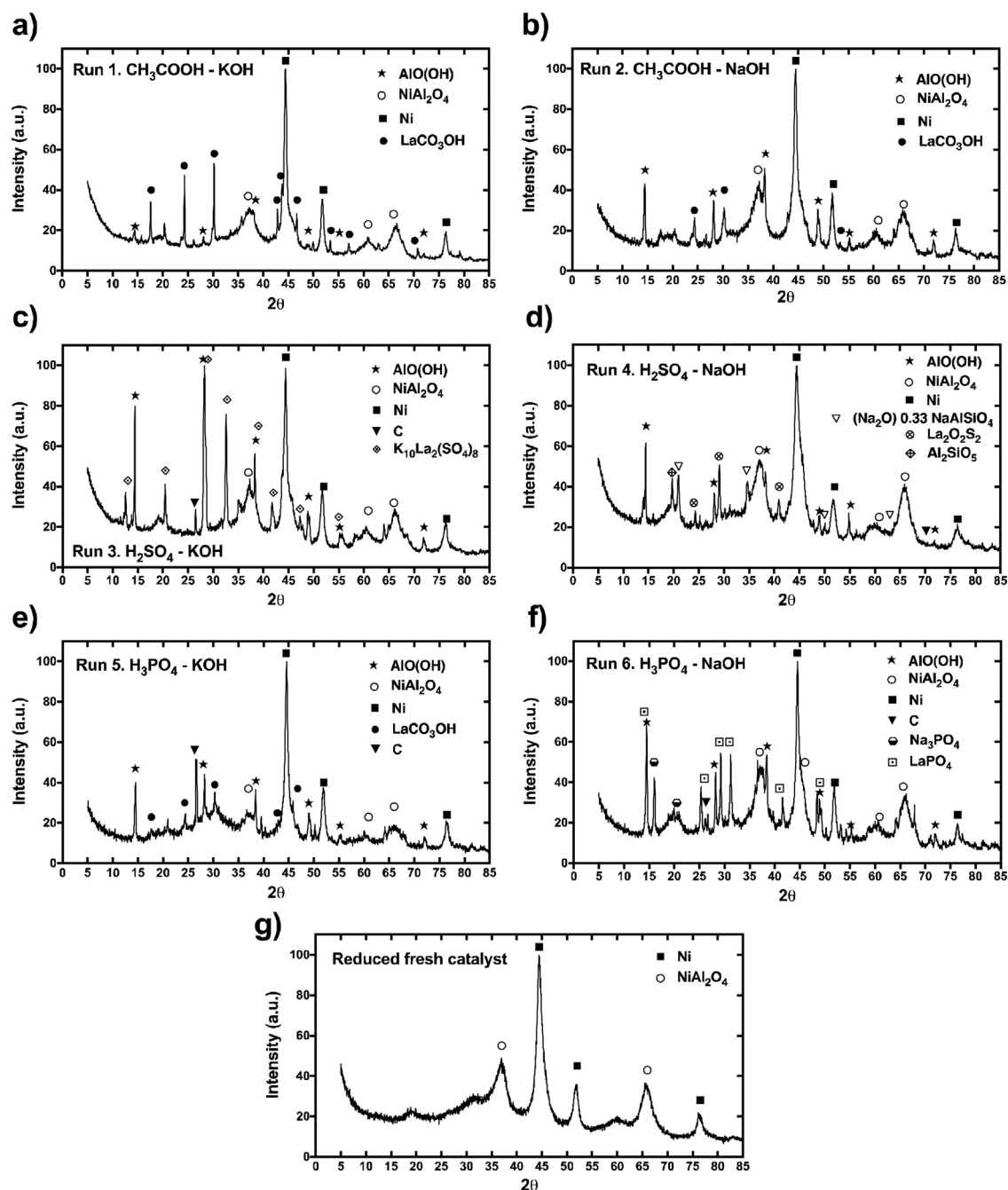


Fig. 5. XRD patterns for the spent catalysts used in the experiments and the reduced fresh Ni-Al-La catalyst.

over time observed in the glycerol conversion and the carbon converted to gas and liquid products for the experiments conducted with  $\text{CH}_3\text{COOH}$  than for those when either  $\text{H}_2\text{SO}_4$  or  $\text{H}_3\text{PO}_4$  were used. This suggests that boehmite formation can partially contribute to catalyst deactivation, but it cannot explain the entire experimental trends observed under the experimental conditions tested in this work, thus indicating the existence of other deactivation mechanisms, especially when  $\text{H}_2\text{SO}_4$  or  $\text{H}_3\text{PO}_4$  are in the glycerol solution.

Fig. 5 shows the XRD patterns of the reduced fresh catalyst and the spent catalyst obtained in each experiment. In the reduced fresh Ni-La/Al catalyst only Ni phases (Ni and  $\text{NiAl}_2\text{O}_4$ ) are detected, suggesting a good dispersion of La on the catalyst structure, while Ni,  $\text{NiAl}_2\text{O}_4$ , and boehmite ( $\text{AlO}(\text{OH})$ ) are crystalline phases detected in all the spent catalysts. This finding confirms that under the

operating conditions of APR, the alumina of the support can be transformed into boehmite [13,20,43], as described above. In addition, other crystalline phases are present in some of the used catalysts depending on the type of acid and base used in the experiments. For the experiments conducted with  $\text{CH}_3\text{COOH}$ , apart from the common phases detected, the presence of  $\text{LaCO}_3\text{OH}$  in the used catalyst can be confirmed regardless of the base used (KOH or NaOH). Moreover, very similar XRD patterns can be observed for the two spent catalysts, and phases of K or Na are not detected. This is consistent with the low amounts of these two elements deposited on both spent catalysts, as described above. In addition, the absence of substantial differences for the amount of C deposited on the catalysts together with the greater  $\text{LaCO}_3\text{OH}$  formation for the experiments conducted with  $\text{CH}_3\text{COOH}$  suggest a lower coke deposition on the catalyst when feeding this impurity in compar-



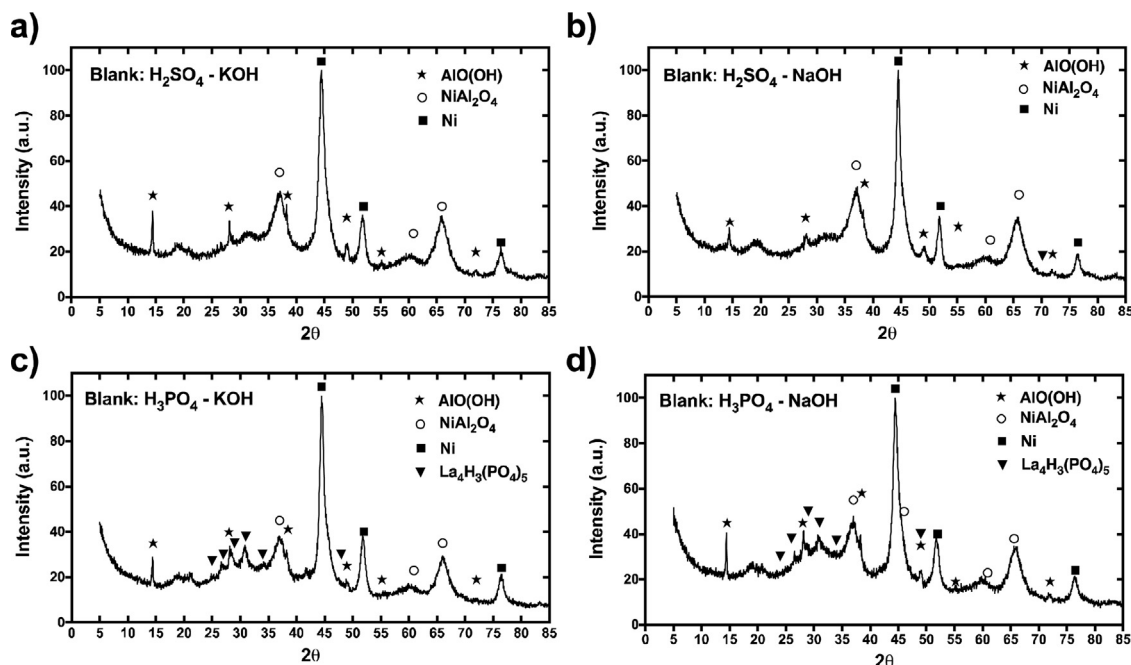


Fig. 6. XRD patterns for the spent catalysts produced in the blank tests.

ison with that produced in the presence of  $\text{H}_2\text{SO}_4$  or  $\text{H}_3\text{PO}_4$ . This development might help to explain the lower deactivation of the catalyst with  $\text{CH}_3\text{COOH}$  than with  $\text{H}_2\text{SO}_4$  or  $\text{H}_3\text{PO}_4$ .

Conversely, a higher number of new crystalline phases, such as  $\text{K}_{10}\text{La}_2(\text{SO}_4)_8$ ,  $(\text{Na}_2\text{O})_0.33\text{NaAlSiO}_4$ ,  $\text{Na}_3\text{PO}_4$  and  $\text{LaPO}_4$ , are detected for the spent catalysts used in the experiments conducted with  $\text{H}_2\text{SO}_4$  and  $\text{H}_3\text{PO}_4$ ; thus showing a greater modification of the crystalline structure of the catalyst than that observed for  $\text{CH}_3\text{COOH}$  during the APR experiments. This development might also account for the lower catalyst deactivation occurring with  $\text{CH}_3\text{COOH}$  than that observed with either  $\text{H}_2\text{SO}_4$  or  $\text{H}_3\text{PO}_4$ , and it also suggests that boehmite formation is not principally responsible for the catalyst deactivation observed in this work. In addition, for  $\text{H}_2\text{SO}_4$  and  $\text{H}_3\text{PO}_4$ , the modification of the crystalline phases of the catalyst depends on the type of base used, i.e. KOH and NaOH, accounting for a more severe phase modification occurring with the latter than with the former base. This also suggests that the incorporation of K in the catalyst occurs without forming new crystalline phases. Conversely, the presence of Na in the glycerol solution promotes catalyst deactivation, aiding the formation of new S and P crystalline phase on the catalyst structure. Very interestingly, the reduction observed over time for the carbon conversion to liquid and the glycerol conversion between the experiments conducted with KOH and NaOH for both  $\text{H}_2\text{SO}_4$  and  $\text{H}_3\text{PO}_4$  are not as different as might have been expected given the great difference in the amounts of K and Na deposited. As the deposition of K occurs to a greater extent and without creating new crystalline phases, this might indicate that either the modification of the crystalline structure of the catalyst exerts a greater effect on catalyst deactivation than poisoning and/or fouling, or that catalyst deactivation could be compensated for by K promoting activity, thus exerting a balancing effect.

To gain a deeper insight into the modification of the crystal phases of the spent catalyst, several blank tests were carried out. In particular, experiments were conducted under the same operating conditions, feeding the inorganic impurities ( $\text{H}_2\text{SO}_4$ ,  $\text{H}_3\text{PO}_4$ , KOH and NaOH) in the absence of glycerol and methanol. Fig. 6 shows the XRD patterns of the spent catalysts produced in the blank tests. Ni,  $\text{NiAl}_2\text{O}_4$ , and boehmite ( $\text{AlO}(\text{OH})$ ) are crystalline phases

detected in all the spent catalysts produced in all the blank tests. The comparison between the blanks and experiments conducted with glycerol/methanol for  $\text{H}_2\text{SO}_4$  (either with KOH or NaOH) reveals the formation of fewer new crystalline phases for the latter than for the former runs. This trend also applies for  $\text{H}_3\text{PO}_4$ . However, for this impurity new phases containing P are observed for the blank conducted with NaOH, although the intensity of the new phases is much lower than for the experiment conducted with glycerol/methanol. These developments might indicate that glycerol and/or glycerol decomposition products (either liquids and/or gases) in the presence of these inorganic impurities exert a greater influence on the modification of the catalyst structure than the inorganic impurities alone, thus suggesting the existence of synergistic effects between the impurities and the organics fed/produced that contribute to catalyst deactivation.

#### 4. Conclusions

This work analyses and compares, under the same operating conditions (220 °C and 44 bar with a Ni-La/Al<sub>2</sub>O<sub>3</sub> catalyst and a  $W/m_{\text{glycerol}}$  ratio of 25 g glycerol min/g catalyst), the effects of some of the most common acid ( $\text{CH}_3\text{COOH}$ ,  $\text{H}_2\text{SO}_4$ ,  $\text{H}_3\text{PO}_4$ ) and basic (KOH and NaOH) biodiesel-derived impurities on the aqueous phase reforming (APR) of a 30 wt.% glycerol solution. The most relevant conclusions are summarised as follows.

1. The impurities considered in this work do not significantly influence the APR of glycerol (before catalyst deactivation) under the operating conditions tested. Specifically, non-statistically significant differences were found for the initial glycerol conversion, carbon conversion and the composition of the liquid phase produced in the experiments with the different acid and bases tested.
2. The impurities exerted a significant influence on catalyst deactivation, resulting in different evolutions over time for the CC gas, CC liq and X gly and the composition of the liquid phase, the catalyst deactivation being as follows:  $\text{H}_3\text{PO}_4$  (KOH = NaOH) >  $\text{H}_2\text{SO}_4$  (KOH < NaOH) >  $\text{CH}_3\text{COOH}$  (KOH < NaOH). The characterisation of the spent catalyst and the liquid phase revealed that poison-

ing/fouling, and catalyst active phase or support modification (leaching and phase transformation), were mainly responsible for the deactivation of the catalyst.

3. The proportion of metals leached from the catalyst (Ni, Al and La) was relatively low and the type of acid and base employed did not affect the amounts leached. Conversely, significant variations were detected for the amounts of K, Na, S and P deposited on the catalysts. In addition, the structure of the catalyst was altered during the APR reaction: the alumina of the support was transformed into boehmite and new crystalline phases appeared.
4. The most severe catalyst deactivation took place in the presence of  $\text{H}_3\text{PO}_4$  and KOH, which accounts for the greater deposition of P and K on the spent catalyst. Conversely, the lowest catalyst deactivation occurred in the presence of  $\text{CH}_3\text{COOH}$  and KOH coinciding with the lowest K deposition and a high boehmite formation.

## Acknowledgements

The authors wish to express their gratitude to the Aragon Government (GPT group), European Social Fund and the Spanish MINECO (projects ENE2010-18985 and ENE2013-41523-R) for providing financial support. The authors would also like to acknowledge the use of the Servicio General de Apoyo a la Investigación-SAI of the Universidad de Zaragoza. In addition, Javier Remón Núñez would like to express his gratitude to the Spanish MINECO for the FPI grant (BES- 2011-044856) awarded.

## References

- [1] R. Manosak, S. Limpattayanate, M. Hunsom, Sequential-refining of crude glycerol derived from waste used-oil methyl ester plant via a combined process of chemical and adsorption, *Fuel Process. Technol.* 92 (2011) 92–99.
- [2] B. Dou, Y. Song, C. Wang, H. Chen, Y. Xu, Hydrogen production from catalytic steam reforming of biodiesel byproduct glycerol: issues and challenges, *Renew. Sustain. Energy Rev.* 30 (2014) 950–960.
- [3] J.M. Silva, M.A. Soria, L.M. Madeira, Challenges and strategies for optimization of glycerol steam reforming process, *Renew. Sustain. Energy Rev.* 42 (2015) 1187–1213.
- [4] D.L. King, L. Zhang, G. Xia, A.M. Karim, D.J. Heldebrant, X. Wang, T. Peterson, Y. Wang, Aqueous phase reforming of glycerol for hydrogen production over Pt–Re supported on carbon, *Appl. Catal. B* 99 (2010) 206–213.
- [5] Y.-C. Lin, Catalytic valorization of glycerol to hydrogen and syngas, *Int. J. Hydrogen Energy* 38 (2013) 2678–2700.
- [6] M. Metsovit, K. Paraskevaidi, A. Koutinas, A.-P. Zeng, S. Papanikolaou, Production of 1,3-propanediol, 2,3-butanediol and ethanol by a newly isolated *Klebsiella oxytoca* strain growing on biodiesel-derived glycerol based media, *Process Biochem.* 47 (2012) 1872–1882.
- [7] Z. Yuan, J. Wang, L. Wang, W. Xie, P. Chen, Z. Hou, X. Zheng, Biodiesel derived glycerol hydrogenolysis to 1,2-propanediol on Cu/MgO catalysts, *Bioresour. Technol.* 101 (2010) 7099–7103.
- [8] A. Iriondo, J.F. Cambra, V.L. Barrio, M.B. Gúemez, P.L. Arias, M.C. Sanchez-Sanchez, R.M. Navarro, J.L.G. Fierro, Glycerol liquid phase conversion over monometallic and bimetallic catalysts: effect of metal, support type and reaction temperatures, *Appl. Catal. B* 106 (2011) 83–93.
- [9] K. Lehnert, P. Claus, Influence of Pt particle size and support type on the aqueous-phase reforming of glycerol, *Catal. Commun.* 9 (2008) 2543–2546.
- [10] A.O. Menezes, M.T. Rodrigues, A. Zimmaro, L.E.P. Borges, M.A. Fraga, Production of renewable hydrogen from aqueous-phase reforming of glycerol over Pt catalysts supported on different oxides, *Renew. Energy* 36 (2011) 595–599.
- [11] D.Ö. Özgür, B.Z. Uysal, Hydrogen production by aqueous phase catalytic reforming of glycerine, *Biomass Bioenergy* 35 (2011) 822–826.
- [12] J.W. Shabaker, G.W. Huber, J.A. Dumesic, Aqueous-phase reforming of oxygenated hydrocarbons over Sn-modified Ni catalysts, *J. Catal.* 222 (2004) 180–191.
- [13] G. Wen, Y. Xu, H. Ma, Z. Xu, Z. Tian, Production of hydrogen by aqueous-phase reforming of glycerol, *Int. J. Hydrogen Energy* 33 (2008) 6657–6666.
- [14] Y. Guo, X. Liu, M.U. Azmat, W. Xu, J. Ren, Y. Wang, G. Lu, Hydrogen production by aqueous-phase reforming of glycerol over Ni–B catalysts, *Int. J. Hydrogen Energy* 37 (2012) 227–234.
- [15] N. Luo, K. Ouyang, F. Cao, T. Xiao, Hydrogen generation from liquid reforming of glycerol over Ni–Co bimetallic catalyst, *Biomass Bioenergy* 34 (2010) 489–495.
- [16] R.L. Manfro, A.F. da Costa, N.F.P. Ribeiro, M.M.V.M. Souza, Hydrogen production by aqueous-phase reforming of glycerol over nickel catalysts supported on  $\text{CeO}_2$ , *Fuel Process. Technol.* 92 (2011) 330–335.
- [17] J. Shabaker, Aqueous-phase reforming of methanol and ethylene glycol over alumina-supported platinum catalysts, *J. Catal.* 215 (2003) 344–352.
- [18] D. Roy, B. Subramaniam, R.V. Chaudhari, Aqueous phase hydrogenolysis of glycerol to 1,2-propanediol without external hydrogen addition, *Catal. Today* 156 (2010) 31–37.
- [19] M.M. Rahman,  $\text{H}_2$  production from aqueous-phase reforming of glycerol over Cu–Ni bimetallic catalysts supported on carbon nanotubes, *Int. J. Hydrogen Energy* 40 (2015) 14833–14844.
- [20] N. Luo, X. Fu, F. Cao, T. Xiao, P.P. Edwards, Glycerol aqueous phase reforming for hydrogen generation over Pt catalyst—effect of catalyst composition and reaction conditions, *Fuel* 87 (2008) 3483–3489.
- [21] A. Seretis, P. Tsiakaras, Hydrogenolysis of glycerol to propylene glycol by in situ produced hydrogen from aqueous phase reforming of glycerol over  $\text{SiO}_2$ – $\text{Al}_2\text{O}_3$  supported nickel catalyst, *Fuel Process. Technol.* 142 (2016) 135–146.
- [22] J. Remón, J.R. Giménez, A. Valiente, L. García, J. Arauzo, Production of gaseous and liquid chemicals by aqueous phase reforming of crude glycerol: influence of operating conditions on the process, *Energy Convers. Manage.* 110 (2016) 90–112.
- [23] J. Remón, C. Jaraute-Córdoba, L. García, J. Arauzo, Analysis and optimisation of  $\text{H}_2$  production from crude glycerol by steam reforming using a novel two step process, *Fuel Process. Technol.* 145 (2016) 130–147.
- [24] J.F. Sierra-Cantor, C.A. Guerrero-Fajardo, Methods for improving the cold flow properties of biodiesel with high saturated fatty acids content: a review, *Renew. Sustain. Energy Rev.* 72 (2017) 774–790.
- [25] D.A. Boga, F. Liu, P.C.A. Bruijninx, B.M. Weckhuysen, Aqueous-phase reforming of crude glycerol: effect of impurities on hydrogen production, *Catal. Sci. Technol.* 6 (2016) 134–143.
- [26] J. Remón, J. Ruiz, M. Oliva, L. García, J. Arauzo, Effect of biodiesel-derived impurities (acetic acid, methanol and potassium hydroxide) on the aqueous phase reforming of glycerol, *Chem. Eng. J.* 299 (2016) 431–448.
- [27] J. Remón, J. Ruiz, M. Oliva, L. García, J. Arauzo, Cheese whey valorisation: production of valuable gaseous and liquid chemicals from lactose by aqueous phase reforming, *Energy Convers. Manage.* 124 (2016) 453–469.
- [28] M. Hajek, F. Skopal, Treatment of glycerol phase formed by biodiesel production, *Bioresour. Technol.* 101 (2010) 3242–3245.
- [29] S.N. Delgado, D. Yap, L. Vivier, C. Especel, Influence of the nature of the support on the catalytic properties of Pt-based catalysts for hydrogenolysis of glycerol, *J. Mol. Catal. A* 367 (2013) 89–98.
- [30] I. Gandarias, P.L. Arias, J. Requies, M.B. Güemez, J.L.G. Fierro, Hydrogenolysis of glycerol to propanediols over a Pt/ASA catalyst: the role of acid and metal sites on product selectivity and the reaction mechanism, *Appl. Catal. B* 97 (2010) 248–256.
- [31] A. Wawrzetz, B. Peng, A. Hrabar, A. Jentys, A.A. Lemonidou, J.A. Lercher, Towards understanding the bifunctional hydrodeoxygenation and aqueous phase reforming of glycerol, *J. Catal.* 269 (2010) 411–420.
- [32] L. Zhang, A.M. Karim, M.H. Engelhard, Z. Wei, D.L. King, Y. Wang, Correlation of Pt–Re surface properties with reaction pathways for the aqueous-phase reforming of glycerol, *J. Catal.* 287 (2012) 37–43.
- [33] J. Remón, V. Mercado, L. García, J. Arauzo, Effect of acetic acid, methanol and potassium hydroxide on the catalytic steam reforming of glycerol: thermodynamic and experimental study, *Fuel Process. Technol.* 138 (2015) 325–336.
- [34] T. Ma, J. Ding, R. Shao, W. Xu, Z. Yun, Dehydration of glycerol to acrolein over Wells–Dawson and Keggin type phosphotungstic acids supported on MCM-41 catalysts, *Chem. Eng. J.* 316 (2017) 797–806.
- [35] T. Miyazawa, Y. Kusunoki, K. Kunimori, K. Tomishige, Glycerol conversion in the aqueous solution under hydrogen over Ru/C+ an ion-exchange resin and its reaction mechanism, *J. Catal.* 240 (2006) 213–221.
- [36] M.C. Martín-Torre, G. Ruiz, B. Galán, J.R. Viguri, Generalised mathematical model to estimate Zn, Pb Cd, Ni, Cu, Cr and As release from contaminated estuarine sediment using pH-static leaching tests, *Chem. Eng. Sci.* 138 (2015) 780–790.
- [37] L. Meng, J. Qu, Q. Guo, K. Xie, P. Zhang, L. Han, G. Zhang, T. Qi, Recovery of Ni, Co, Mn, and Mg from nickel laterite ores using alkaline oxidation and hydrochloric acid leaching, *Sep. Purif. Technol.* 143 (2015) 80–87.
- [38] J. Remón, L. García, J. Arauzo, Cheese whey management by catalytic steam reforming and aqueous phase reforming, *Fuel Process. Technol.* 154 (2016) 66–81.
- [39] H. Al-Sheeha, M. Marafi, A. Stanislaus, Reclamation of alumina as boehmite from an alumina-supported spent catalyst, *Int. J. Miner. Process.* 88 (2008) 59–64.
- [40] A.M.d.A. Cruz, J. Guillaume Eon, Boehmite-supported vanadium oxide catalysts, *Appl. Catal. A* 167 (1998) 203–213.
- [41] J. Yang, Y. Zhao, R.L. Frost, Surface analysis, TEM, dynamic and controlled rate thermal analysis, and infrared emission spectroscopy of gallium doped boehmite nanofibres and nanosheets, *Appl. Surf. Sci.* 255 (2009) 7925–7936.
- [42] Y. Yang, Y. Xu, B. Han, B. Xu, X. Liu, Z. Yan, Effects of synthetic conditions on the textual structure of pseudo-boehmite, *J. Colloid Interface Sci.* 469 (2016) 1–7.
- [43] M. El Doukkali, A. Iriondo, J.F. Cambra, I. Gandarias, L. Jalowiecki-Duhamel, F. Dumeignil, P.L. Arias, Deactivation study of the Pt and/or Ni-based  $\gamma$ - $\text{Al}_2\text{O}_3$  catalysts used in the aqueous phase reforming of glycerol for  $\text{H}_2$  production, *Appl. Catal. A* 472 (2014) 80–91.